8

Experimental Study for Condensation Heat Transfer Inside Helical Coil

Mohamed A. Abd Raboh[1], Hesham M. Mostafa[2],
Mostafa A. M. Ali[2] and Amr M. Hassaan[3]
[1]*Faculty of Engineering, Al Azhar University,*
[2]*Faculty of Engineering, King Abdulaziz University,*
[3]*Higher Technological Institute, Tenth of Ramadan City,*
[1,3]*Egypt*
[2]*K.S.A*

1. Introduction

Heat exchangers are one of the most common technological devices applied in refrigeration, air-conditioning, nuclear power generation, petrochemical, pharmaceutical, aerospace industries and food processing industries. Many options are available for obtaining compactness and efficiency in exchanging thermal power. In the field of tubular heat exchangers one possible way for reducing the space occupied by the exchanger is by bending tube axis in helicoidal shape. This option is particularly suitable when construction simplicity is needed and when the geometry of the place in which the exchanger has to be housed is the cylindrical one. Many advantages derive from this disposition, such as an excellent behavior in presence of severe thermal expansions; in fact the helical shape allows the exchanger to behave as a spring, thus accommodating the stresses due to the expansions. Helicoidal pipes have been extensively studied and used in a variety of engineering areas due to their high efficiency in heat transfer and compactness in volume. Han et al. [1] investigated the condensation heat transfer and pressure drop characteristics of R-134a in an annular helical pipe. The obtained results show that the refrigerant-side condensation heat transfer coefficients and pressure drops of R-134a increase with the mass flux of R-134a. The saturated temperatures have significant effects on the condensation heat transfer coefficients of R-134a in the annular helical pipe. Lin and Ebadian [2] investigated the condensation heat transfer and pressure drop of R-134a in annular helicoidal pipe at different orientations. The results shows that, the effect of individual parameter revealed that the refrigerant Nusselt number was larger at lower refrigerant saturation temperature, and would increase with the increase of mass flow rates of both refrigerant and cooling water. When the orientation increased from 0 degree to 90 degree, the percentage increase of refrigerant Nusselt number from 0 degree to 45 degree accounted for more than two times of that from 45 degree to 90 degree. Han et al. [3] investigate the condensation heat transfer of R-134a flow inside helical pipes at different orientations. The obtained results show that, the condensation heat transfer coefficient from the refrigerant side for the helical pipe at the inclined position is the highest, and the vertical position is the lowest. Laohalertdecha and Wongwises [4] studied the effect of corrugation pitch on the condensation heat transfer coefficient and pressure

drop of R-134a inside horizontal corrugated tube. Murai et al. [5] studied structure of air–water two-phase flow in helically coiled tubes. The obtained results shows that, owing to the curvature of the tube, which provides centrifugal acceleration to the two-phase flow, the flow transition from bubbly to plug flow is considerably quickened compared to that in the flow in a straight tube. Also, in comparison with an upward inclined straight tube, small bubbles vanish away from the liquid slug in the case of a strong curvature owing to the centrifugal acceleration. Wongwises and Polsongkram [6] investigated the condensation heat transfer and pressure drop of R-134a in a helically coiled concentric tube-in-tube heat exchanger. Their obtained results show that, the average heat transfer coefficient increases with increasing average vapor quality and mass flux. The heat transfer coefficient increases very slightly with an increase in heat flux. On the contrary, it decreases with increasing saturation temperature. Li and Ji-tian [7] investigated the condensation heat transfer of R-134a in horizontal straight and helically tube in tube heat exchanger. Their results show that, the average heat transfer coefficient for the helical section is 4%-13.8% higher than that for the straight section. M. Moawed [8] investigated the forced convection from helical coiled tubes with different parameters**.** Their results showed that, for the same P/do, the higher values of Nusselt number (Nu_m) can be obtained with a high value of D/do while the small value of Nu_m can be obtained with a small value of D/do. Al-Hajeri et al. [9] investigated heat transfer performance during condensation of R-134a inside helicoidal tubes. Their experimental results show that, the average heat flux, refrigerant side heat transfer coefficient and overall heat transfer coefficients increase with increasing of the mass flux of flowing R-134a. The refrigerant side heat transfer coefficient and overall heat transfer coefficient decrease as the saturation temperature increases. Xin et al. [10] investigated an experimental study of single-phase and two-phase flow pressure drop in annular helicoidal pipes. Wongwises and Polsongkarm [11] investigated the evaporation heat transfer and pressure drop of HFC-134a in a helically coiled concentric tube-in-tube heat exchanger. Condensation of R134a flowing inside helicoidal pipe investigated by Laohalertdecha and Wongwises [12]. Their obtained results show that, the average heat flux of the refrigerant flow increases with the water flow rate.

It is clear from the previous review and up to the knowledge of the authors that, there is a shortage in thesis which concerned with condensation of steam inside helical coil. Accordingly, in this work, an experimental study is done to investigate the effect of different operating parameters on the condensation heat transfer coefficient for steam flows inside helical coil.

2. Experimental test rig

The experimental test rig is illustrated in Fig. 1. It is mainly consists of a circular inlet section, a rectangular cross section duct in which the tested helical coil is installed, and the heating steam loop. Air is drawn from the ambient by the blower 2.5 hp rated power (2). A flexible connection (3) separates the blower section and the rest of the wind tunnel to eliminate any vibrations promoted. The leaving air from the blower flows through a velocity meter (8) to measure the average air velocity inside the wind tunnel.

Wind tunnel (4) walls are made of galvanized iron sheet of 1 mm thick. The basic dimensions for the wind tunnel are 2.5 m long, 670 mm wide and 330 mm high. Tested helical coil with different dimensions is fitted, vertical or inclined, at the middle of the test section, as shown in Fig. (1). To insure that a fully developed flow is achieved at the entrance of the test section (7), air is traveled through the entrance region (6) of 2 m long,

which having the same rectangular cross section as that of the test section. Also, outlet air flows through bell mouth which installed at the exit section of the wind tunnel.

The helical coil was tested inside the wind tunnel at different operating parameters. The tested operating parameters are; pipe diameter, coil diameter, coil pitch, and coil orientations. All tested helical coils have the same outer surface area (0.1 m^2). Five values of inner diameters of pipe are tested; 3.36, 4.95, 11.3, 14.48 and 17.65 mm. The tested helical coil was wrapped at five different coil diameters as; 100, 125, 150, 200, and 250 mm. Also; the helical coil was formed at different coil pitches (20, 30, 40, and 50 mm). The tested helical coil orientations are vertical (90 degree) and inclined positions with different angles (30, 45, 60 degree). The outer surfaces of the tunnel walls are completely insulated with 30 mm glass wool to minimize the heat loss.

Heating steam loop consists of electric boiler and water separator. The basic dimensions of the electric boiler are 0.4 m in diameter and 0.6 m height. Two electric heaters (each one 1.5 kW rated power) are used. Each electric element is controlled through automatic switch with max load of 20 A; to protect the boiler from over load hazards and to control the required amount of heating steam. Safety valve was set to 3 bar and fixed at the upper port of the boiler. Also, pressure gauge was fit to the boiler upper port to monitor the steam pressure inside the boiler. The steam line includes a back pressure valve (10) to assure the steady stream flow with a selected heating steam pressure , a regulator (11) to control the amount of steam mass flow rate needed. The generated steam from electric boiler is naturally moved to water separator and leaves it in dry saturated condition. Then, heating steam passes through the helical coil and it is condensed inside it. The steam condensate is collected in a calibrated glass tube in a certain time to measure the condensate flow rate, and a thermocouple is fit to the condensate line to measure the condensate temperature outlet from tested helical coil.

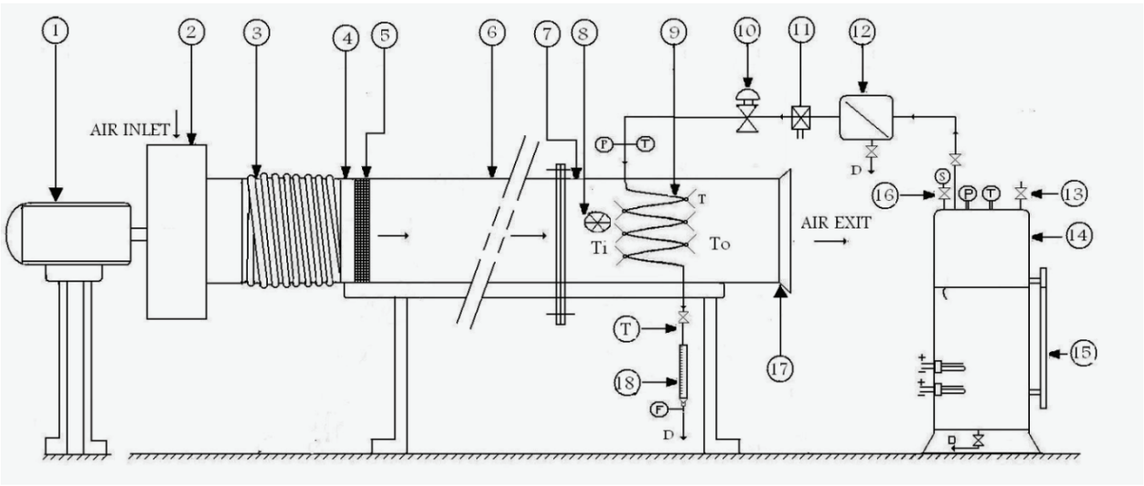

1-	Electric motor	8-	Velocity meter	15-	Level indicator
2-	Blower	9-	Test helical coil	16-	Safety valve
3-	Flexible connection	10-	Back pressure valve	17-	Exit bill mouse
4-	Wind tunnel	11-	Regulator	18-	Burette
5-	Screen	12-	Water separator	D	Drain
6-	Entrance region	13-	Vent valve	F	Flow rate
7-	Entrance test section	14-	Electric boiler	P	Pressure
				T	Temperature

Fig. 1. Schematic diagram of the experimental test rig

3. Measurements and methodology

The experimental measurements are taken to determine the condensation heat transfer coefficient for the steam which flows inside helical coil. Prior to start of the experiments, the electric boiler filled with suitable volume of water. Glass level indicator was fixed in the side of the boiler to monitor the water level inside the boiler. The generated steam moves into the water separator to get it dry saturated steam. The steam was getting out from the water separator to the back pressure valve to get the suitable pressure which needed in the experiment. Then the regulator control the required amount of steam passed to the tested helical coil to condense inside it due to air flowing inside the wind tunnel on the outer surface of the coil. The experimental test rig is allowed to operate until the fluctuation in temperatures was about ±0.1 ^{o}C. Then, steady state condition is reached. Once the test rig is reached to the desired steady state condition, the required measurements of temperature, pressure and volume flow rate are taken. Temperatures of inlet heating steam at inlet and condensate outlet from each tested helical coil are measured. Surface temperature, inlet and outlet air temperatures and other temperatures in different positions are measured by using 0.5 mm copper-constantan thermocouple (type k), which connected to a temperature recorder via multi point switch having an accuracy of ± 0.1 ^{o}C. The uncertainty in temperature measurements is ±0.1 ^{o}C. Due to the small amount of condensate from coil a calibrated constant volume tank and stop watch is used. Inlet steam pressure is measured by Bourdon pressure gauge with minimum readable value of ± 0.05 bar. Air velocity was measured by a hot wire anemometer sensor (type Testo 605-V1, of 8mm probe diameter), with a resolution of 0.01 m/s. The root-mean-square random error propagation analysis is carried out in the standard fashion using the measured experimental uncertainties of the basic independent parameters. The experimental uncertainties associated with these measurements technique are estimated to be approximately less than 12 % for condensation heat transfer coefficient.

4. Data reduction

The basic measurements are analyzed using a computer reduction program to calculate the condensation heat transfer coefficient. At steady state, the total input heat from the heating steam which flows inside the helical coil (Q_{st}) can be transferred to the flowing air inside wind tunnel. It is divided into useful heat to air (Q_{air}) and the remaining amount of heat transferred to the surroundings as heat loss (Q_{loss}). The total input heat can be determined as follow;

$$Q_{st} = \dot{m}_{st}(i_g - i_o) \tag{1}$$

Where;

$\dot{m}_{st}$: Steam flow rate inside helical coil, kg/s.

i_g : Specific enthalpy for dry saturated steam evaluated at the steam inlet pressure to the tested coil, J/kg.

i_o : Specific enthalpy for condensate at the outlet from test coil, J/kg.

The useful heat transfer to air flow inside the wind tunnel can be calculated from measuring mass flow rate which flow inside the helical coil and the temperature rise in the air as;

$$Q_{air} = \dot{m}_{air} Cp_{air} \left(T_{air,o} - T_{air,i}\right) \tag{2}$$

Where:

$\dot{m}_{air}$: Mass flow rate of air in the wind tunnel, kg/s.
Cp_{air} : Specific heat of air, J/kg ^{o}C.
$T_{air,i}$: Inlet air temperature, ^{o}C.
$T_{air,o}$: Outlet air temperature, ^{o}C.
Then, the amount of heat loss from the test section to the surrounding (Q_{loss}) can be determined as the difference between input heat and useful heat as;

$$Q_{loss} = Q_{st} - Q_{air} \tag{3}$$

Heat flux (q") can be calculated from the following equation as;

$$q" = Q_{st} / A_{s,i} \tag{4}$$

Where;
$A_{s,i}$: Inner surface area of the pipe forming the tested helical coil, ($A_{s,i} = \pi d_i L$).
d_i : Inner pipe diameter, m.
L : Pipe length, m.
Accordingly, the condensation heat transfer coefficient (h_c) can be calculated as;

$$h = q" / \left(T_{sat} - T_{s,i}\right) \tag{5}$$

Where:
T_{sat} : Saturation temperature for heating steam, ^{o}C.
$T_{s,i}$: Average value for the inner surface temperature of the pipe, ^{o}C.
Reynolds number can be defined as:

$$\mathrm{Re} = \frac{4 * \dot{m}_{st}}{\pi d_i \mu} \tag{6}$$

Where:
μ: dynamic viscosity of steam at average bulk temperature.
The average values for the Nusselt number (Nu), could be evaluated as,

$$Nu = \frac{h * d_i}{k} \tag{7}$$

Where, k: Thermal conductivity for working fluid.

5. Results and discussion

Appropriate analysis for the experimental measurements; lead to obtain the heat flux and condensation heat transfer coefficient for different operating parameters. The studied operating conditions are pipe diameter, coil diameter, coil pitch, and coil orientations. All tested helical coils have the same outer surface area (0.1 m^2).

5.1 Effect of inner pipe diameter

The variation of heat flux versus temperature difference for different values of inner pipe diameters (di =3.36, 4.95, 11.3, 14.48 and 17.65 mm) at vertical position with coil pitch (P =30 mm) are shown in figures (2). It is observed that, for all the studied coil diameters (100, 125, 150, 200 and 250 mm), heat flux increases with decreasing inner pipe diameter until it reach

to the maximum value at inner pipe diameter equal to 4.95 mm. Then it decreases with decreasing inner pipe diameter to 3.36 mm due to capillary effects. Also, heat flux increases with increasing temperature difference. Therefore the optimum value for inner pipe diameter was found to be 4.95 mm.

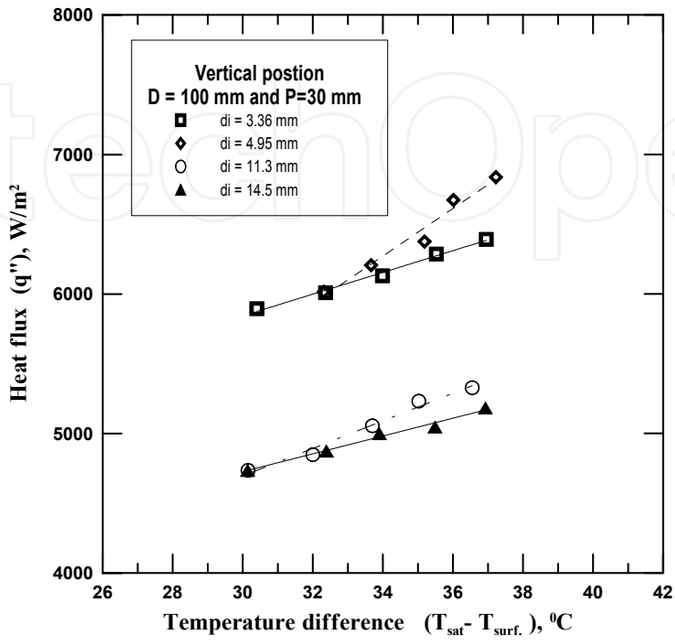

Fig. 2a. Heat flux versus temperature difference for different inner pipe diameters at P =30 mm and D =100 mm.

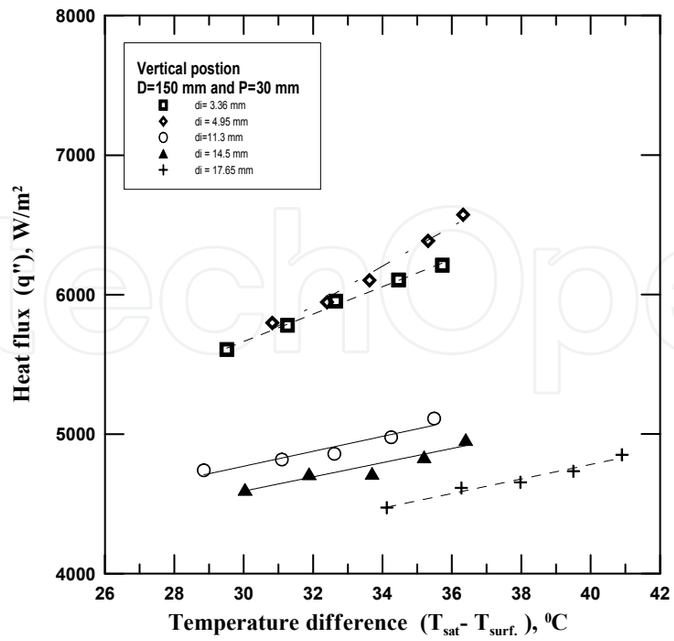

Fig. 2b. Heat flux versus temperature difference for different inner pipe diameters at P =30 mm and D =150 mm.

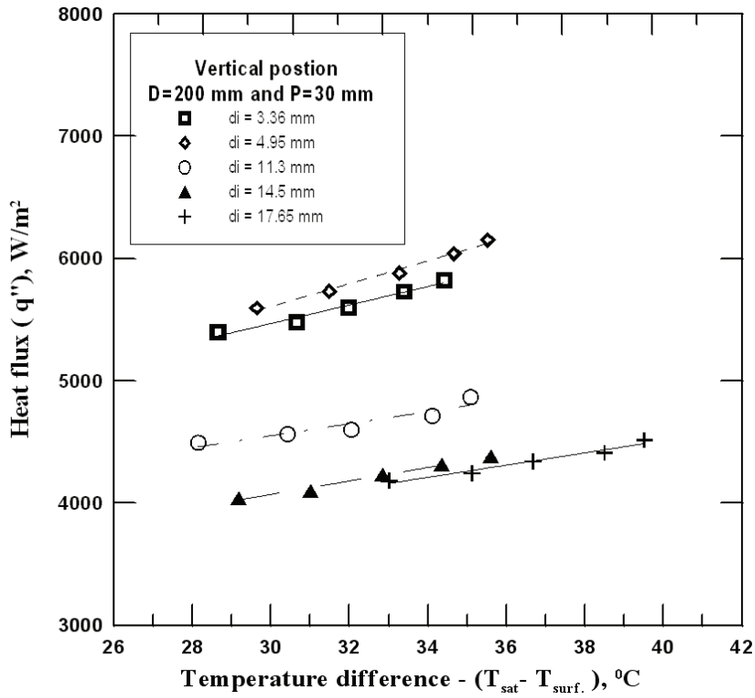

Fig. 2c. Heat flux versus temperature difference for different inner pipe diameters at P =30 mm and D =200 mm.

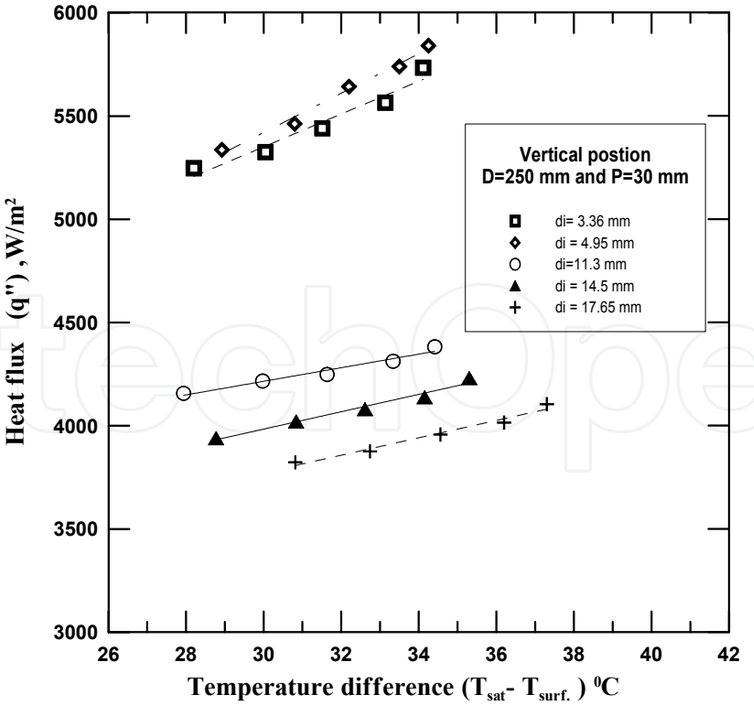

Fig. 2d. Heat flux versus temperature difference for different inner pipe diameters at P =30 mm and D =250 mm.

5.2 Effect of coil diameter

The variation of heat flux versus temperature difference for different values of coil diameters (100, 125, 150, 200 and 250 mm) at vertical position with coil pitch (P =30 mm) are shown in figures (3). It is observed that, for all the studied inner pipe diameters (di =3.36, 4.95, 11.3, 14.48 and 17.65 mm), heat flux increases with decreasing coil diameter. Also, heat flux increases with increasing temperature difference. This can be attributed to the air flows faster around the small coil diameter which give more cooling to the coil surface. Therefore the optimum value for coil diameter was found to be 100 mm.

5.3 Effect of coil pitch

The variation of heat flux versus temperature difference for different values of coil pitches (P= 20, 30, 40 and 50 mm) at vertical position with coil diameter (D =100 mm) and inner pipe diameter (di =4.95 mm) is shown in Fig. (4). It is observed that, for the optimum values of coil diameter and inner pipe diameter, heat flux increases with increasing coil pitch until it reach to the maximum value at coil pitch equal to 40 mm. This can be explained as the flow of air increases between the turns of the coil which give more cooling to the coil surface. But increasing coil pitch than 40 mm leads to the coil takes more flat shape accordingly heat flux decreases with increasing coil pitch (as shown in figure at 50 mm). Therefore the optimum value for coil pitch was found to be 40 mm.

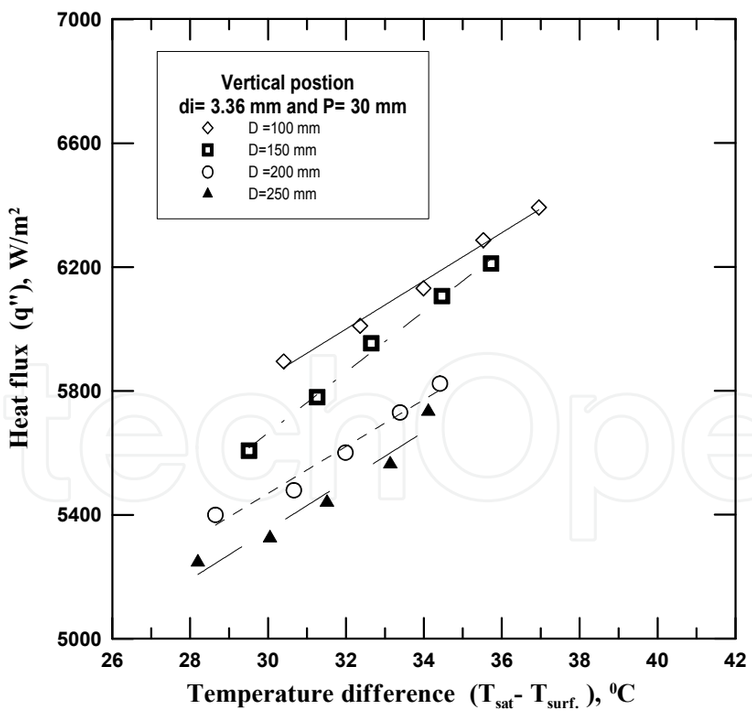

Fig. 3a. Heat flux versus temperature difference for different coil diameters at P =30 mm and di =3.36 mm.

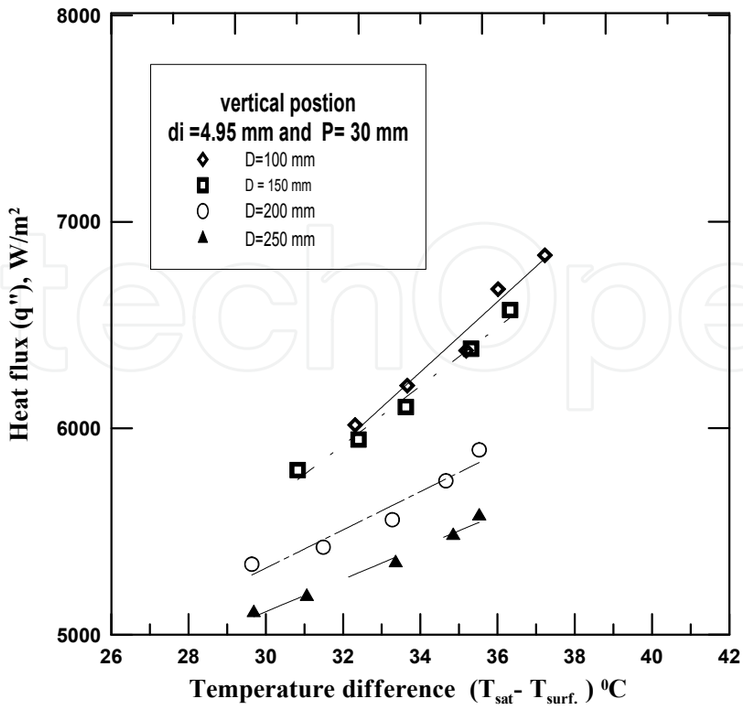

Fig. 3b. Heat flux versus temperature difference for different coil diameters at P =30 mm and di =4.95 mm.

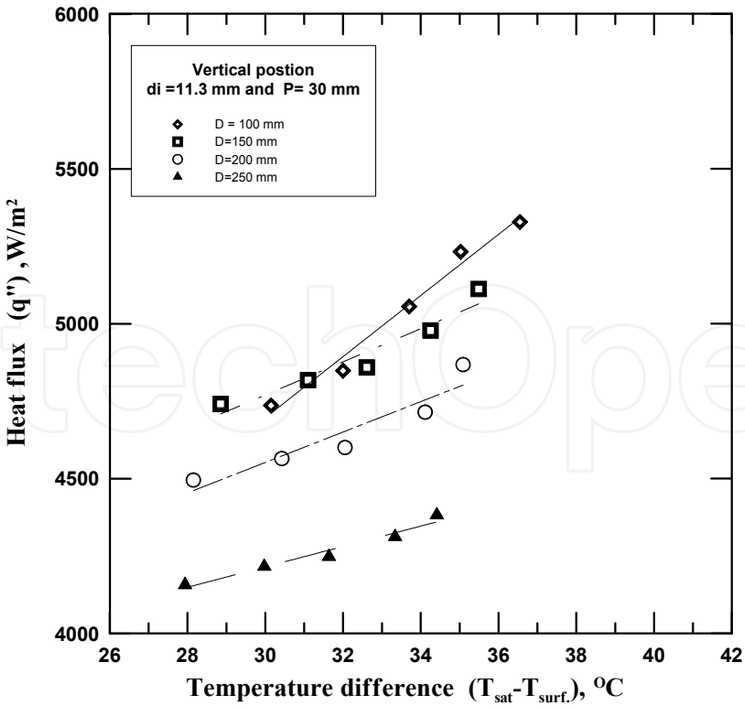

Fig. 3c. Heat flux versus temperature difference for different coil diameters at P =30 mm and di =11.3 mm.

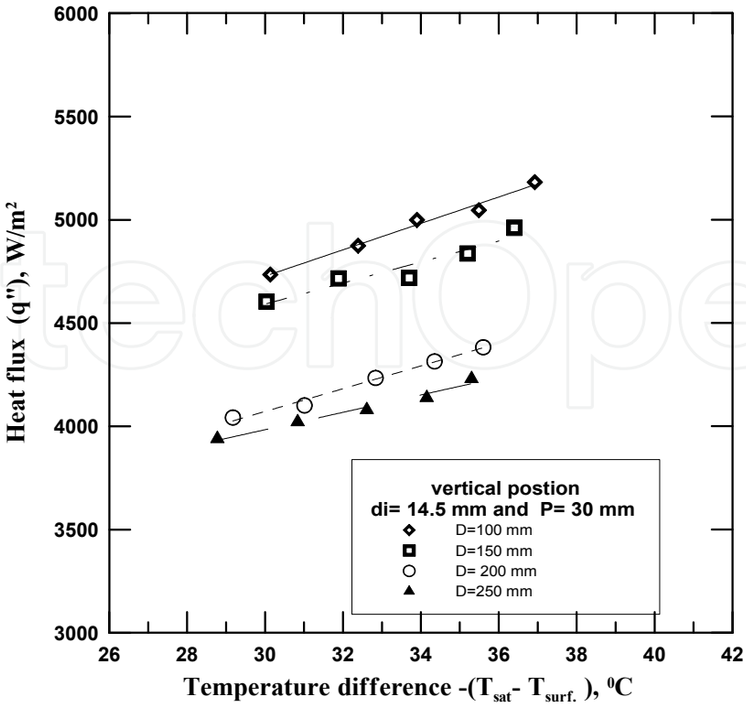

Fig. 3d. Heat flux versus temperature difference for different coil diameters at P =30 mm and di =14.48 mm.

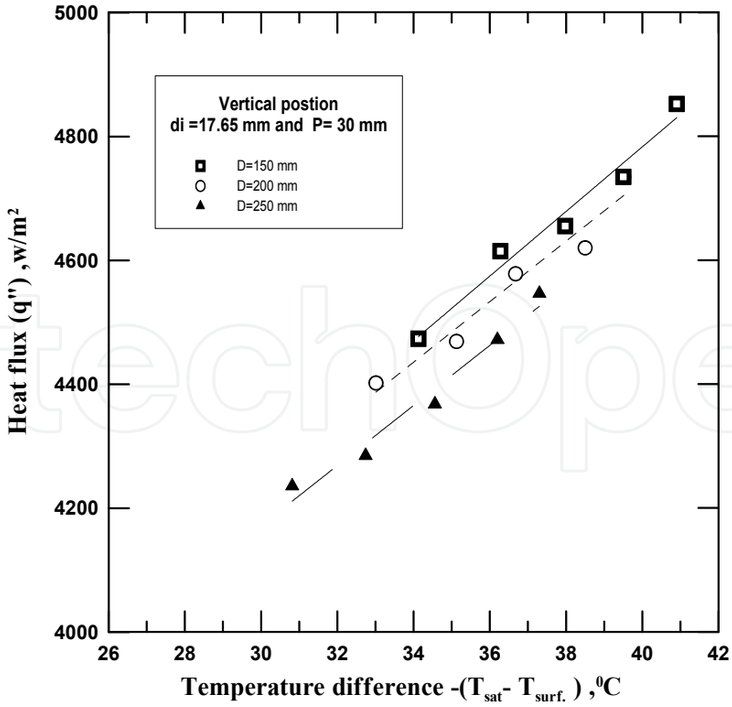

Fig. 3e. Heat flux versus temperature difference for different coil diameters at P =30 mm and di =17.65 mm.

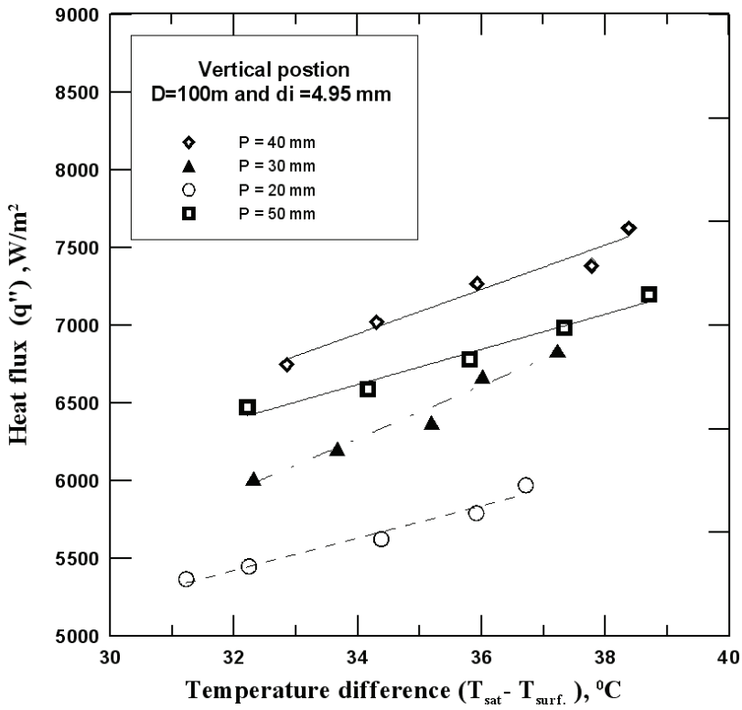

Fig. 4. Heat flux versus temperature difference for different coil pitches at d_i =4.95 mm and D =100 mm.

5.4 Effect of coil orientations

The variation of heat flux versus temperature difference for different coil orientations at inner pipe diameter (di =4.95 mm), coil diameter (D =100 mm) and coil pitch (P= 40 mm) is shown in figure (5). It is observed that heat flux increases with decreasing inclination angle from 90 degree up to 45 degree it reaches to the maximum value. This can be attributed due to the air can hit the inner surfaces for every turn of helical coil resulting a decrease in the average surface coil temperature. Accordingly, the amount of condensate increases and then the heat flux increases. The resultant of decreasing surface temperature and increase in heat flux, cause an increase in the condensation heat transfer coefficient. Also, it is observed that heat flux decreases with decreasing angle than 45 degree (as shown in figure at 30 degree) due to reduction in flow capability for the working fluid inside the pipe. Therefore the optimum inclination angle was 45 degree.

Also, a comparison between two inner diameters for vertical and inclined with 45 degree was illustrated in Fig. (6), for D=100 mm, P=40 mm. As mentioned above small diameter (d_i=4.95 mm) gave higher values for heat flux. Therefore it is concluded that, the optimum operating parameters in the studied operating range are; d_i =4.95 mm, D=100 mm, P=40 mm, and inclination angle for coil 45 degree.

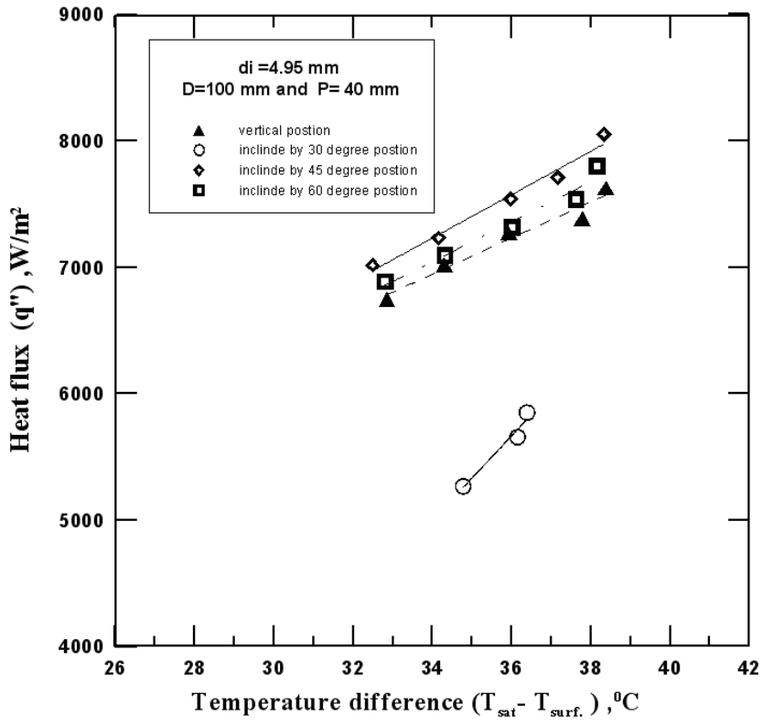

Fig. 5. Heat flux versus temperature difference for different coil orientations at di=4.95 mm, D =100 mm and P =40 mm

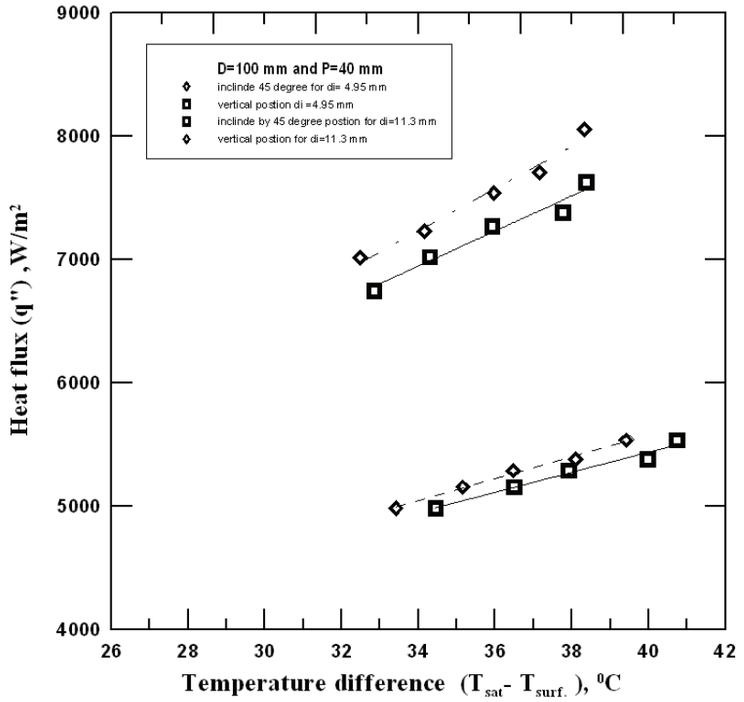

Fig. 6. Heat flux versus temperature difference for two inner diameters in vertical and inclined positions (45 degree) at D =100 mm and P=40 mm.

5.5 Condensation heat transfer coefficient

The variation of heat flux versus saturation temperature for different values of L/d_i at D =100 mm are shown in Fig. (7). It is observed that, heat flux increases with increasing saturation temperature. Also, heat flux takes higher values for L/d_i =1012; which corresponding to the coil which have the inner diameter; d_i=4.95 mm and length; L=5.01 m.

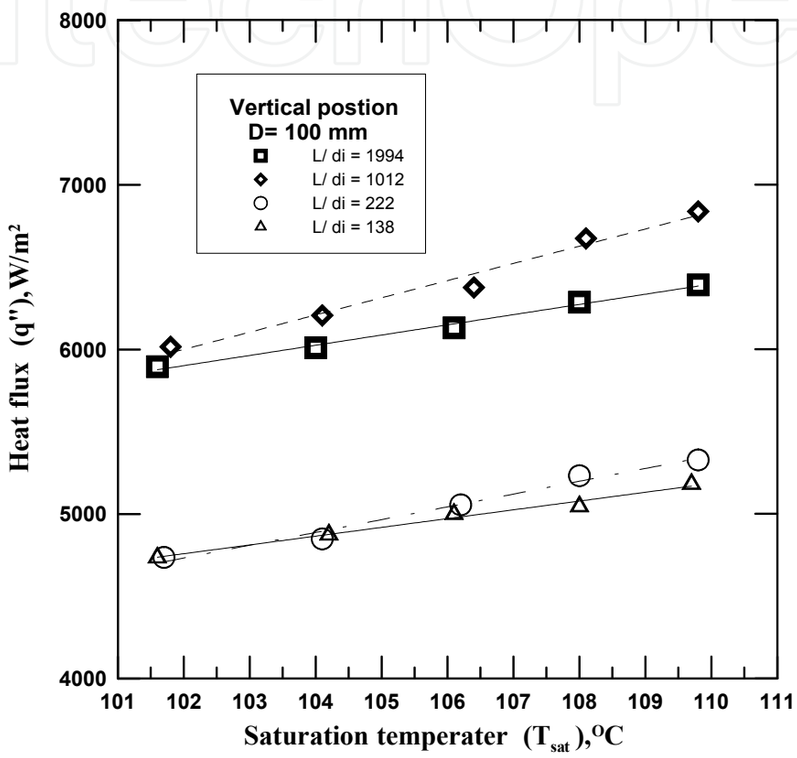

Fig. 7. Heat flux versus saturation temperature for different L/d_i at D =100 mm

Figure (8) illustrates the condensation heat transfer coefficient versus saturation temperature for different values of L/d_i at D =100 mm and P=30 mm. It is observed that, condensation heat transfer coefficient decreases with increasing saturation temperature. This can be pertained as increasing saturation temperature cause an increase in both surface temperature and heat flux. But the increase in temperature difference more dominant than the increase in heat flux. Also, condensation heat transfer coefficient takes higher values for L/d_i =1012.

Figure (9) illustrates the condensation heat transfer coefficient versus L/d_i at D =100, 150, 250 mm and P=30 mm for vertical position. It is found that, condensation heat transfer coefficient takes higher values for L/d_i =1012 as illustrated in Fig. (8) which corresponds to the coil inner diameter; d_i=4.95 mm and length; L=5.01 m.

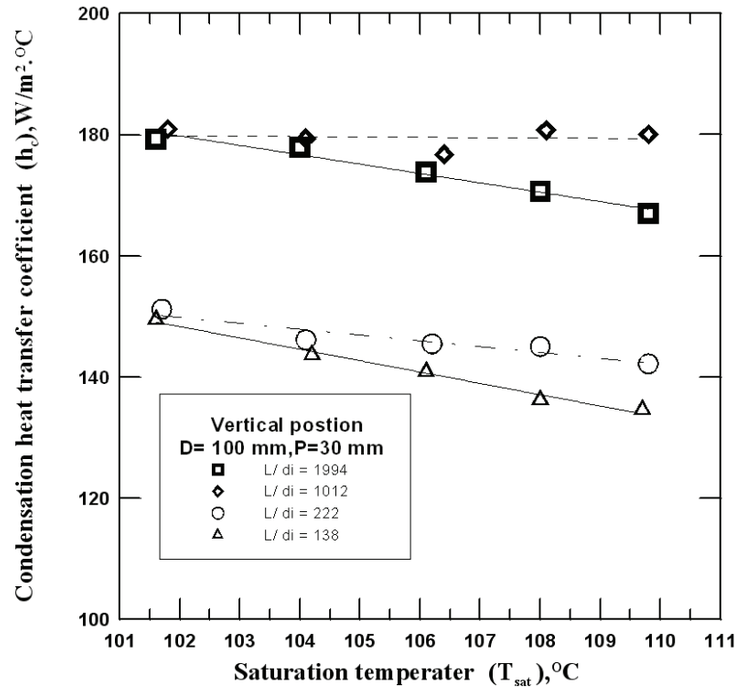

Fig. 8. Condensation heat transfer coefficient versus saturation temperature for different L/d_i at D =100 mm.

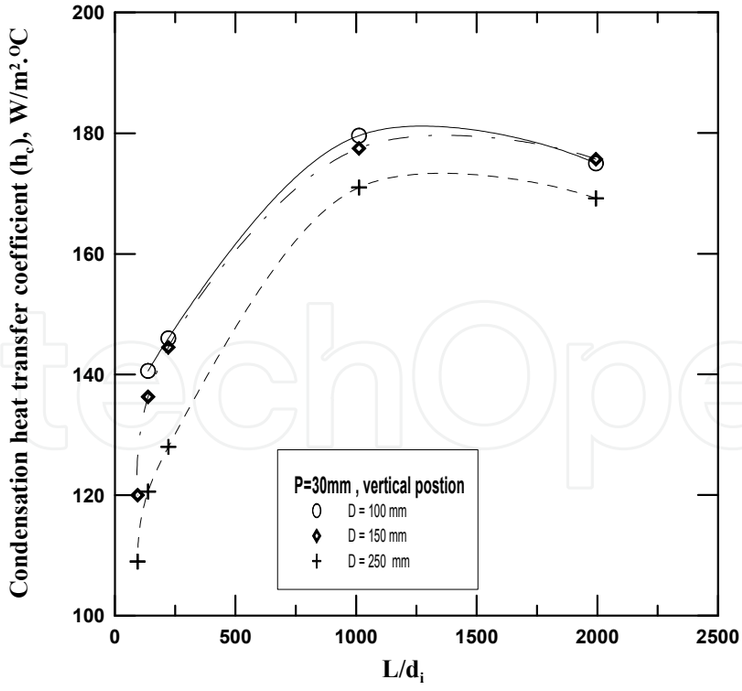

Fig. 9. Condensation heat transfer coefficient versus L/d_i ratio.

Condensation heat transfer coefficient versus P/d_i for vertical position at L/d_i =1012 and D =100 mm was illustrated in Fig. (10). Condensation heat transfer coefficient increases

gradually with P/d_i as shown in figure and takes the highest value at P/d_i =8.1 which corresponding to the coil Pitch P=40 mm and coil inner diameter; d_i=4.95 mm.
Condensation heat transfer coefficient versus D/d_i for vertical position at P =30 mm was illustrated in Fig. (11). Condensation heat transfer coefficient takes the highest value at D/d_i =20.2 which corresponding to the coil diameter D=100 mm and coil inner diameter; d_i=4.95 mm.

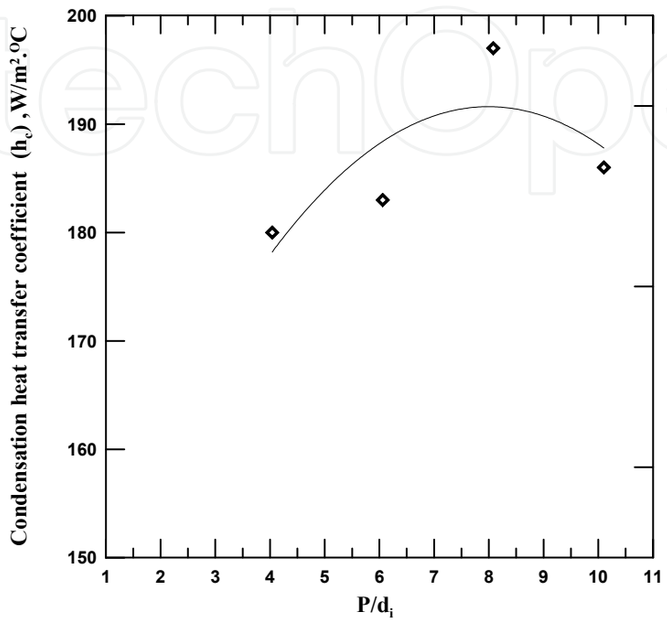

Fig. 10. Condensation heat transfer coefficient versus P/d_i for vertical position at L/d_i =1012 and D =100 mm

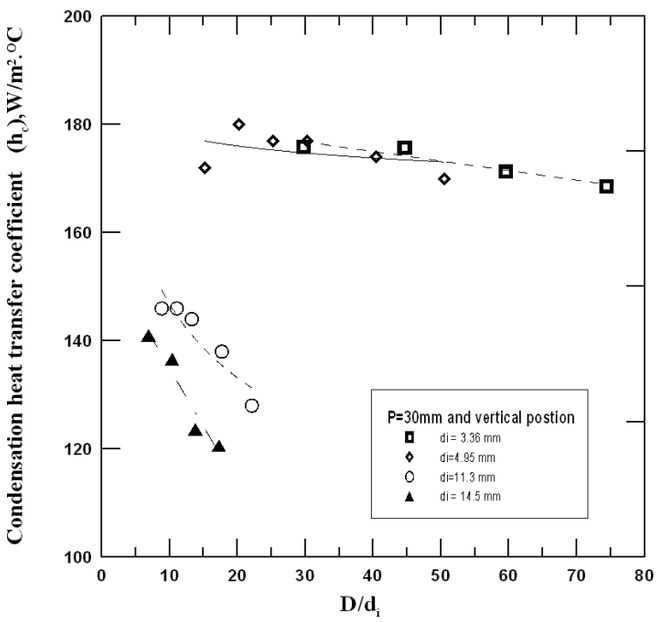

Fig. 11. Condensation heat transfer coefficient versus D/d_i ratio.

Therefore it is concluded that, the optimum dimensionless operating parameters in the studied operating range are; D/d_i =20.2, L/d_i =1012 and P/d_i =8.1 and inclination angle for coil 45 degree.

5.6 Nusselt number

Figure (12) shows the variation of Nusselt number versus Reynolds number for optimum operating parameters (d_i =4.95 mm, D=100 mm, P=40 mm). It is observed that, Nusselt number takes higher values for the optimum inclination angle was 45 degree.

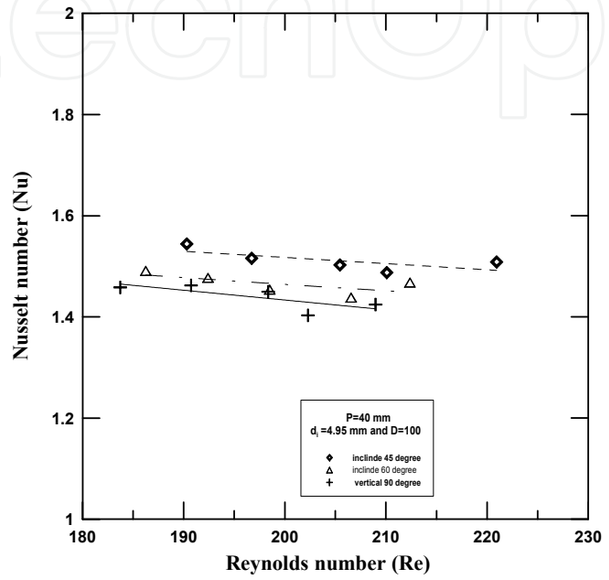

Fig. 12. Nusselt number versus Reynolds number for optimum operating conditions.

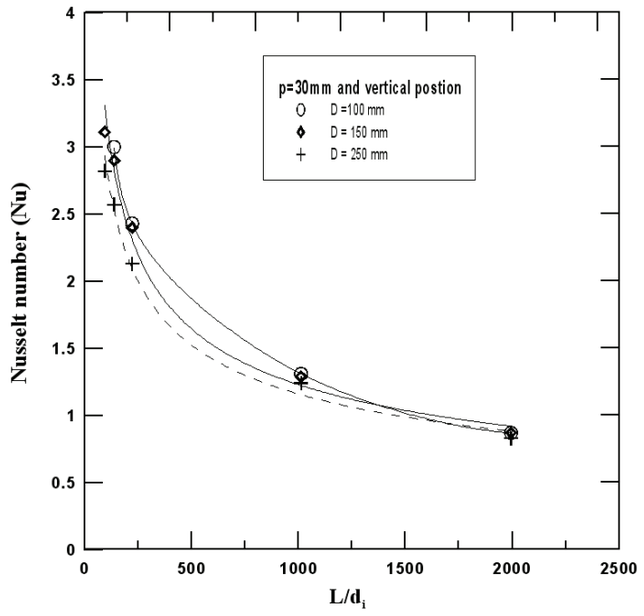

Fig. 13. Nusselt number versus L/d_i ratio.

Figure (13) illustrates the variation of Nusselt number versus versus L/d_i at D =100, 150, 250 mm and P=30 mm for vertical position. It is found that, Nusselt number decreases with increasing L/d_i and take an asymptotic value for L/d_i greater than 1000. Nusselt number versus P/d_i for vertical position at L/d_i =1012 and D =100 mm was illustrated in Fig. (14). Nusselt number takes the highest value at P/d_i =8.1. Nusselt number versus D/d_i for vertical position at P =30 mm was illustrated in Fig. (15). Nusselt number takes the highest value at D/d_i =20.2.

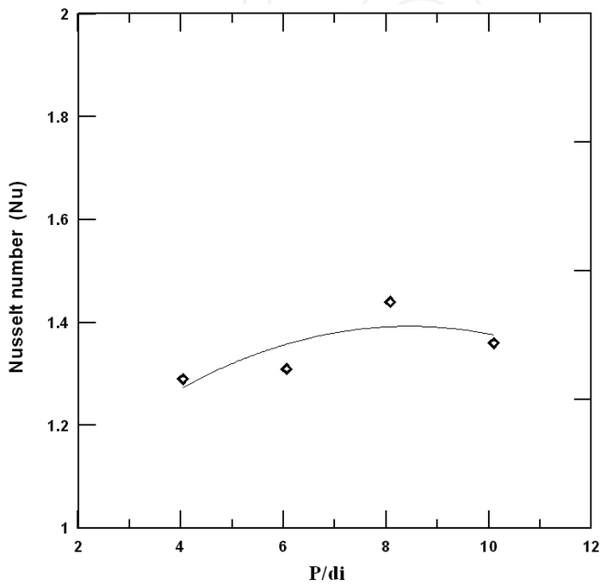

Fig. 14. Nusselt number versus P/d_i for vertical position at L/d_i =1012 and D =100 mm.

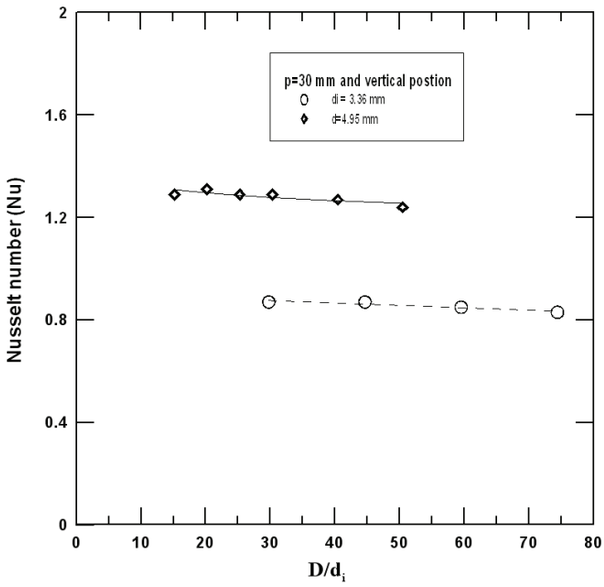

Fig. 15. Nusselt number versus D/d_i ratio.

An empirical correlation for Nusselt number as a function of Reynolds number and the examined operating parameters was derived as:

$$\mathbf{Nu} = \mathbf{8.25}\ \left(\mathbf{Re}\right)^{0.426}\left(\mathbf{D}/\mathbf{d_i}\right)^{-0.1023}\left(\mathbf{P}/\mathbf{d_i}\right)^{0.03245}\left(\mathbf{L}/\mathbf{d_i}\right)^{-0.5352} \quad (8)$$

Figure (16) shows a comparison between the calculated Nusselt number from the proposed correlation and Nusselt number evaluated from the experimental findings. The above correlation is related to the considered operating parameters in this work (40<Re<230, 8.5<D/di<74.4, 1.7<P/di<10.1 and 94.6<l/di<1994). It is clear from figure that, the maximum error in predicted values Nusselt number by the above suggested correlation was found to be nearly ± 20%.

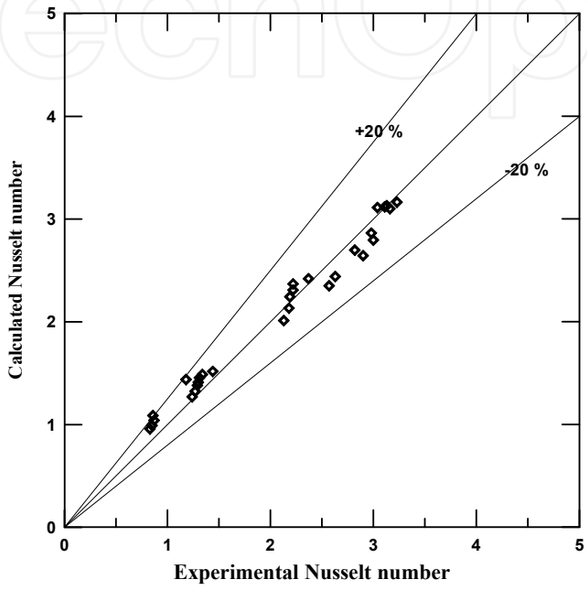

Fig. 16. Comparison between the calculated Nu from the proposed correlation and Nu evaluated from the experimental findings.

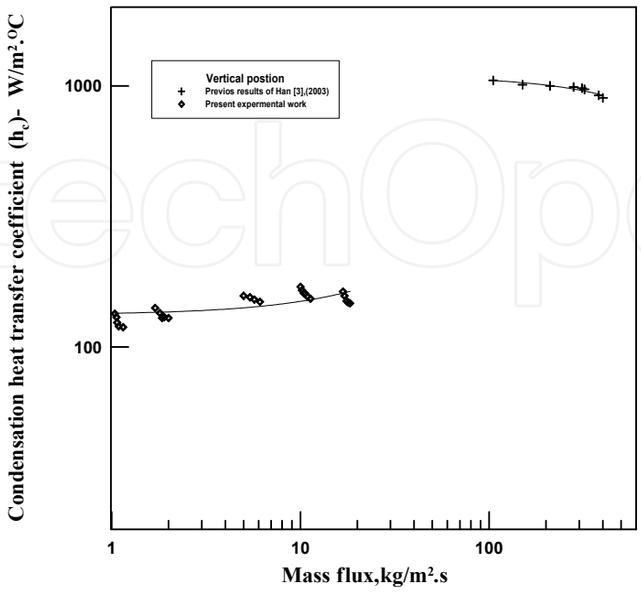

Fig. 17. Comparison with the previous work.

Figure (17) shows a comparison between condensation heat transfer coefficient for the present work and the previous work of Han et al. [3] which studied condensation heat transfer of R-134a flow inside helical pipes at different orientations. It clear from figure that comparison between the present works with the previous work gave fair agreement due to using steam in the present work as a working fluid.

6. Conclusions

Experimental study was conducted to determine the condensation heat transfer of steam which flow inside helical coil. The operating parameters are; pipe diameter, coil diameter, coil pitch, and coil orientations. The obtained experiments results show that;
condensation heat transfer coefficient increases with decreasing saturation temperature. Condensation heat transfer coefficient increases with the decrease pipe diameter and helical coil diameter then it is decreases. Also condensation heat transfer coefficient increases with the increase of coil pitch up to a certain value (p=40 mm) then it is decreases. Condensation heat transfer coefficient takes higher values for inclined position with angle 45^o than the vertical and other inclination angles. Therefore the optimum operating parameters in the studied operating range are; d_i =4.95 mm, D= 100 mm, P=40 mm, and inclination angle for coil 45 degree. Accordingly the optimum dimensionless operating parameters in the studied operating range are; D/d_i =20.2, L/d_i =1012 and P/d_i =8.1. An empirical correlation for Nusselt number as a function of Reynolds number and the examined operating parameters. Comparison between the present works with the previous work gave fair agreement.

7. Nomenclature

A_s : Surface area, m^2.
Cp : Specific heat, J/kg. ^oC
d : Pipe diameter of the helical coil, m
D : Helical coil diameter, m
h : Condensation heat transfer coefficient, W/m^2. ^oC
i : Specific enthalpy, J/kg
k : Thermal conductivity, W/m. ^oC
L : helical coil length, m
$\dot{m}$: Mass flow rate, kg/s
P : Helical coil pitch, m
Nu : Nusselt number, -
Q : Heat transfer rate, W
Re : Reynolds number, -
q" : Heat flux, W/m^2
T : Temperature, ^oC
Greek symbols
μ : Dynamic viscosity, kg/m.s

8. Subscripts

air : air
g : Dry saturated steam

i : inner, inlet
loss : loss
o : outer, outlet
s : surface
st : steam

9. References

[1] J.T. Han, C.X. Lin and M.A. Ebadian "Condensation heat transfer and pressure drop characteristics of R-134a in an annular helical pipe" International Communications in Heat and Mass Transfer 32, (2005), pp. 1307-1316.

[2] C.X. Lin and M.A. Ebadian "Condensation heat transfer and pressure drop of R-134a in annular helicoidal pipe at different orientations" International Journal of Heat and Mass Transfer 50, (2007), pp. 4256–4264.

[3] J.T. Han, H.J. Kang, C.X. Lin, A. Awwad and M.A. Ebadian "Condensation heat transfer of R-134a flow inside helical pipes at different orientations", Int. Comm. Heat Mass Transfer, Vol. 30, no. 6, (2003), pp. 745-754.

[4] S. Laohalertdecha, S. Wongwises "The effects of corrugation pitch on the condensation heat transfer coefficient and pressure drop of R-134a inside horizontal corrugated tube" International Journal of Heat and Mass Transfer, Vol. 53, (2010), pp. 2924–2931.

[5] Y. Murai, S. Yoshikawa, S. Toda , M. Ishikawa and F. Yamamoto "Structure of air–water two-phase flow in helically coiled tubes" Nuclear Engineering and Design, Vol. 236, (2006), pp. 94–106.

[6] S. Wongwises and M. Polsongkram "Condensation heat transfer and pressure drop of HFC-134a in a helically coiled concentric tube-in-tube heat exchanger", International Journal of Heat and Mass Transfer, Vol. 49, (2006), pp. 4386–4398.

[7] S. Li and H. Ji-tian " condensation heat transfer of R-134a in horizontal straight and helically coiled tube-in-tube heat exchangers" Journal of hydrodynamics, Vol. 19, no. 6, (2007), pp. 677-682.

[8] M. Moawed "Experimental study of forced convection from helical coiled tubes with different parameters", Energy Conversion and Management, (2010), inpress

[9] M.H. Al-Hajeri, A.M. Koluib, M. Mosaad and S. Al-Kulaib" Heat transfer performance during condensation of R-134a inside helicoidal tubes" Energy Conversion and Management 48, (2007), pp. 2309–2315.

[10] R.C.Xin, A. Awwad, Z.F. Dong and M.A. Ebadian "Experimental study of single-phase and two-phase flow pressure drop in annular helicoidal pipes" International comn. heat and fluid flow 18, (1997), pp. 483-488.

[11] S. Wongwises, M. Polsongkram " Evaporation heat transfer and pressure drop of HFC-134a in a helically coiled concentric tube-in-tube heat exchanger" International Journal of Heat and Mass Transfer 49, (2006), pp. 658–670.

[12] S. Laohalertdecha, S. Wongwises "The effects of corrugation pitch on the condensation heat transfer coefficient and pressure drop of R-134a inside horizontal corrugated tube" International Journal of Heat and Mass Transfer 53, (2010), pp. 2924–2931.

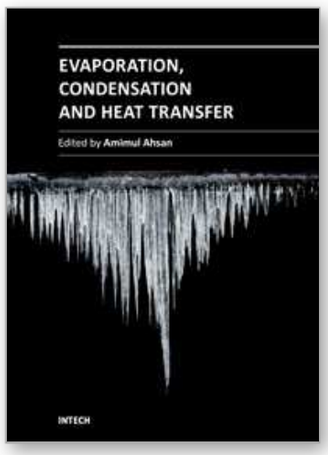

Evaporation, Condensation and Heat transfer
Edited by Dr. Amimul Ahsan

ISBN 978-953-307-583-9
Hard cover, 582 pages
Publisher InTech
Published online 12, September, 2011
Published in print edition September, 2011

The theoretical analysis and modeling of heat and mass transfer rates produced in evaporation and condensation processes are significant issues in a design of wide range of industrial processes and devices. This book includes 25 advanced and revised contributions, and it covers mainly (1) evaporation and boiling, (2) condensation and cooling, (3) heat transfer and exchanger, and (4) fluid and flow. The readers of this book will appreciate the current issues of modeling on evaporation, water vapor condensation, heat transfer and exchanger, and on fluid flow in different aspects. The approaches would be applicable in various industrial purposes as well. The advanced idea and information described here will be fruitful for the readers to find a sustainable solution in an industrialized society.

InTech Europe
University Campus STeP Ri
Slavka Krautzeka 83/A
51000 Rijeka, Croatia
Phone: +385 (51) 770 447
Fax: +385 (51) 686 166
www.intechopen.com

InTech China
Unit 405, Office Block, Hotel Equatorial Shanghai
No.65, Yan An Road (West), Shanghai, 200040, China
中国上海市延安西路65号上海国际贵都大饭店办公楼405单元
Phone: +86-21-62489820
Fax: +86-21-62489821

IntechOpen